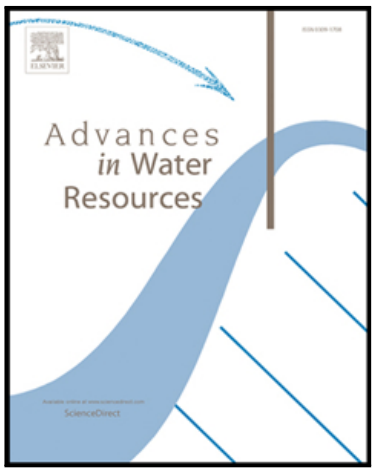

Rising tides, rising gates: the complex ecogeomorphic response of coastal wetlands to sea-level rise and human interventions

Steven Sandi , Jose Rodriguez , Neil Saintilan , Gerardo Riccardi , Patricia Saco

PII: S0309-1708(17)30616-4
DOI: 10.1016/j.advwatres.2018.02.006
Reference: ADWR 3092

To appear in: *Advances in Water Resources*

Received date: 14 June 2017
Revised date: 4 February 2018
Accepted date: 5 February 2018

Please cite this article as: Steven Sandi , Jose Rodriguez , Neil Saintilan , Gerardo Riccardi , Patricia Saco , Rising tides, rising gates: the complex ecogeomorphic response of coastal wetlands to sea-level rise and human interventions, *Advances in Water Resources* (2018), doi: 10.1016/j.advwatres.2018.02.006

Highlights

- Mixed mangrove-saltmarsh wetlands are particularly vulnerable to Sea Level Rise (SLR)
- Tidal attenuation due to man-made structures limits wetland adaptation capacity to SLR
- Dynamic inlet control enhances SLR resilience by preventing mangrove encroachment

Rising tides, rising gates: the complex ecogeomorphic response of coastal wetlands to sea-level rise and human interventions

Steven Sandi[1], Jose Rodriguez[1,2], Neil Saintilan[3], Gerardo Riccardi[4], Patricia Saco[1,2*]

[1] School of Engineering, The University of Newcastle, Callaghan 2308, Australia

[2] Centre for Water Security and Environmental Sustainability, The University of Newcastle

[3] Department of Environmental Sciences, Macquarie University, North Ryde 2109, Australia

[4] Department of Hydraulics and Research Council of National University of Rosario (CIUNR), Rosario 2000, Argentina

[*] Corresponding author

Abstract

Coastal wetlands are vulnerable to submergence due to sea-level rise, as shown by predictions of up to 80% of global wetland loss by the end of the century. Coastal wetlands with mixed mangrove-saltmarsh vegetation are particularly vulnerable because sea-level rise can promote mangrove encroachment on saltmarsh, reducing overall wetland biodiversity. Here we use an ecogeomorphic framework that incorporates hydrodynamic effects, mangrove-saltmarsh dynamics, and soil accretion processes to assess the effects of control structures on wetland evolution. Migration and accretion patterns of mangrove and saltmarsh are heavily dependent on topography and control structures. We find that current management practices that incorporate a fixed gate for the control of mangrove encroachment are useful initially, but soon become ineffective due to sea-level rise. Raising the gate, to counteract the effects of sea level rise and promote suitable hydrodynamic conditions, excludes mangrove and maintains saltmarsh over the entire simulation period of 100 years

Keywords: sea-level rise, coastal wetlands, ecogeomorphic modelling, mangrove, saltmarsh.

1. Introduction

Coastal wetlands support very rich and complex ecosystems, and often function as food sources for terrestrial and aquatic animal species (Abrantes and Sheaves, 2009, Winemiller et

al., 2007, Kelleway et al., 2017), carbon sinks (Macreadie et al., 2017) and sanctuary for endangered species (Kelleway et al., 2017). Both saltmarsh and mangrove can be present in coastal wetlands and, while saltmarshes can be found in different climates around the world, mangroves are mainly restricted to tropical and sub-tropical climates because they are less tolerant to low temperatures (Saintilan and Rogers, 2013) . In SE Australian estuaries, a typical zonation of vegetation communities exists, with a sequence that includes mudflats at the seaward margin, mangrove in the lower and middle areas of the tidal frame and saltmarsh at the upper limit of the tidal frame. Similar vegetation structure can be found on the southeast coasts of US (Armitage et al., 2015) and China (Chen et al., 2016), southern estuaries of Brazil (Spier et al., 2016) and New Zealand (Hayward et al., 1999, Lundquist et al., 2014). The most common species of saltmarshes of SE Australia are *Sarcocornia quinqueflora, Sporobolus virginicus and Juncus krausii* (Boon et al., 2015), while *Avicennia marina* and *Aegiceras corniculatum* are the two dominant species of mangrove.

Tidal regime has been recognized as a critical driver of saltmarsh and mangrove distribution of mixed environments (Spier et al., 2016), and combined with the topography determines inundation extent, water depth, and frequency of inundation. It also influences soil salinity, mangrove propagule establishment and nutrient propagation (Saintilan et al., 2009 and references therein), with high soil salinity in the upper tidal frame reducing the dominance of mangrove (Crase et al., 2013).

Like many coastal areas around the world, Australian coastal wetlands are under development pressure. This pressure not only includes the direct removal of vegetation due to land-use changes, but also the effect of flow barriers and control structures that alter the natural tidal patterns. Wetland management and rehabilitation under such conditions is challenging. Many rehabilitation projects have focussed on improving mangrove areas, a practice that can affect other habitats because mangroves are an invasive and persistent species (Straw and Saintilan, 2006). Mangrove encroachment on saltmarsh environments shows a general trend worldwide at higher latitudes (Saintilan et al., 2014), and in numerous estuaries of SE Australia has led to a broad reduction of shorebird habitat (Saintilan and Williams, 1999).

Coastal wetlands are also vulnerable to submergence due to sea-level rise, as shown by predictions of up to 80% of global wetland loss by the end of the century (Craft et al., 2009,

Day et al., 2008, Morris et al., 2002, Kirwan et al., 2010, van Wijnen and Bakker, 2001). Sea-level rise effects on mixed mangrove-saltmarsh wetlands can be even more serious, because it can accelerate mangrove encroachment on saltmarsh. This is the case of SE Australia, where recent studies estimate a significant saltmarsh loss over the next decades due to both mangrove encroachment and sea-level rise, particularly in the absence of buffer areas for inland migration of saltmarsh (Oliver et al., 2012, Rogers et al., 2012). The ecological significance of mangrove and saltmarsh environments is widely recognized, but in a mixed environment, saltmarsh reduction due to mangrove colonization can have significant impact in the wetland biodiversity. In SE Australia, saltmarsh are important habitats of waterbirds and bats (Kelleway et al., 2017), as well as other species of mammals, reptiles and amphibians (Saintilan and Rogers, 2013). Mangrove habitat is preferred by fish communities, but the impacts that mangrove encroachment on saltmarsh has on fish population are still uncertain (Kelleway et al., 2017). In fact, invertebrates that live on saltmarsh are a major food source for some fish species (Saintilan and Rogers, 2013).

Human intervention through hydraulic manipulation of tidal inputs is a common practice in coastal areas around the world for a number of purposes including agriculture, mosquito control and land reclamation (Gedan et al., 2009 and references therein). For instance, the coastal wetlands of SE Australia have been greatly affected by modifications to tidal flows mostly for agriculture, with more than 4000 tidal flow restrictions identified in the New South Wales coast alone (Williams and Watford, 1997). Most of these modifications are designed to limit tidal flow, but hydraulic manipulation can also be used to restore wetlands. In particular, flow restrictions have been shown to provide an effective control mechanism for mangrove encroachment into saltmarsh (Rodríguez and Howe, 2013). However, their longer term effects on wetland vegetation dynamics under sea-level rise are still unclear and have not been adequately investigated.

Previous research has shown that wetland evolution includes complex ecogeomorphic interactions between hydrodynamic conditions, vegetation establishment and soil accretion processes (Morris et al., 2002; D'Alpaos and Marani, 2016;, Krauss et al., 2014; Belliard et al., 2016; Passeri et al., 2015, Saco and Rodríguez, 2013 and references therein). It has also shown the importance of including attenuation effects due to human intervention when predicting wetland evolution under increasing sea levels (Rodríguez et al., 2017). Here we analyse the complex response of a mangrove-saltmarsh wetland to the combined effects of

sea-level rise and human intervention using an ecogeomorphic simulation approach that includes tidal propagation and attenuation effects. Different management intervention strategies are analysed, which consist of including control gates at the wetland inlet to limit mangrove encroachment on saltmarsh. We study three different viable scenarios: a baseline scenario without a gate and two different operation scenarios for the control gate, one with a fixed height compatible with current sea-level and one with a variable height following predicted sea-level changes. These set of simulations allow for a novel and improved understanding of the complex relation between hydrodynamic changes, vegetation migration and soil accretion and provide valuable insight for future management of wetlands under sea-level rise. The intervention strategies explored herein are in line with conservation management practices currently in use in SE Australian wetlands, where mangrove encroachment on saltmarsh is an important issue to be considered during sea-level rise. Other approaches that promote natural bio-geomorphic processes considering increases in sediment supply have been shown to have potential for improving wetland resilience to sea-level rise in other parts of the world (Temmerman et al., 2013, Temmerman and Kirwan, 2015). However, our previous research has shown that the use of bio-geomorphic based strategies alone will not significantly improve the fate of SE Australian wetlands under sea-level rise (Rodríguez et al., 2017).

2. Study site

The Hunter Estuary in New South Wales is one of the most important sites for migratory shorebirds species in Australia. Human interventions have occurred in the estuary since the 1850s. In the particular case of Kooragang Island (Fig.1), drains and levees were implemented in order to make the area suitable for industrial and grazing purposes. In 1993, the Kooragang Wetland Rehabilitation Project (KWRP) was established for management and maintenance of the wetlands (Williams et al., 2000) and part of the KWRP included the removal of control structures in order to reinstate tidal flows to an enclosed experimental site named as Area E (Fig.1). Area E is located approximately 10.5 km upstream from the mouth of the Hunter River. It has a total area of approximately 1.24 km^2. Inflows into Area E come from the South Arm of the Hunter River via two inlets: Wader Creek and Fish Fry Creek inlet. Changes to the tidal regime resulted in important changes in the vegetation distribution and shorebird habitat availability. The reinstated tidal flows produced an initial increase of saltmarsh areas, but promoted conditions for mangroves to colonize lower mudflat and

saltmarsh areas in the following years. This encroachment resulted in a reduction of shorebird habitat (Howe et al., 2010).

The Hunter estuary exhibits a semi-diurnal tidal cycle with a tidal range of about 1.6 m. Runoff flows from the Hunter River are one order of magnitude less than the tidal flow and only 20% of this flow is distributed via the South arm (Fig. 1a); therefore, the tide is the main hydrologic driver of the flow delivered to the study site. The wetland in Area E is divided into four major compartments by a series of earthworks and culverts (Fig. 1b). Fish Fry Creek receives flow directly from the Hunter River and can be considered a non-attenuated compartment, since water levels fluctuate following the semidiurnal tide in the estuary with minimum modifications. Wader Creek is a semi-attenuated compartment because it receives inflows both from the Hunter River via a culvert, and from an overland connection with Fish Fry Creek that becomes active when water levels overtop an internal embankment during high tides. The culvert located at Wader Creek inlet is heavily constricted and only a small fraction (1%) of tidal flows are conveyed via this inlet. The other two compartments located further inland are Wader Pond and Swan Pond. Flows entering these compartments and the connectivity between them are heavily attenuated by culverts. Sediment influx from the Hunter Estuary is the main source of suspended particle matter in Area E, as higher concentrations have been reported in locations near the inlets (Howe, 2008).

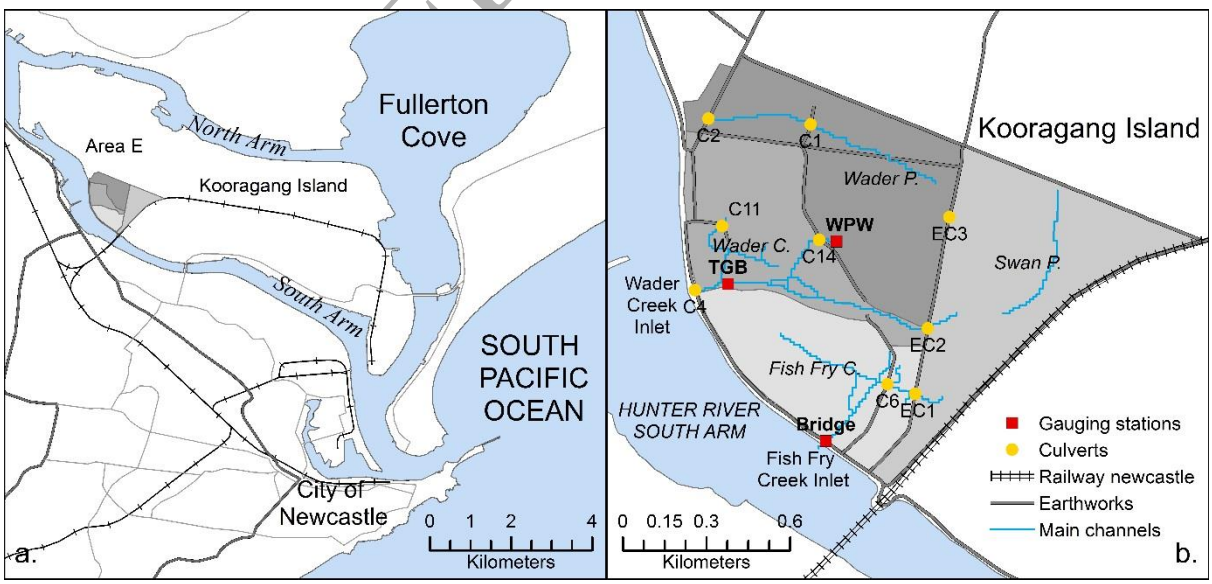

Figure 1. Location of the study site and Area E subdivision and control structures.

Vegetation survey of Area E shows that the study site has most of the estuarine habitats present in the Hunter Estuary (Howe, 2008, Howe et al., 2009), including mudflats, tidal pools, mangrove and saltmarsh. Mangrove forests consist of homogenous and dense populations of Grey Mangrove (*A. Marina*) and saltmarshes are dominated by Beaded Samphire (*S. quinqueflora*) and Marine Couch (*S. virginicus*) (Rodríguez and Howe, 2013). The confinement imposed by an outer perimeter with high embankments is clearly one of the major problems in Area E because mangrove encroachment on saltmarsh is expected to continue (Rodríguez and Howe, 2013) while saltmarsh landward migration is restricted by the outer embankments. Due to internal compartmentalization, there is no clear zonation in relation to elevation in Area E. Mudflats and pools, saltmarsh, and mangroves are observed in the same elevation range in most of the wetland (Supp. Figs. 1, 2).

Since the initial stages of mangrove invasion at the site, wetland managers have sought ways of reducing mangrove cover and restoring saltmarsh. Previous research has shown that mangrove establishment in the short term can be controlled with the use of a flood gate at the Fish Fry Creek inlet (Howe, 2008). However, the long term sustainability of tidal manipulation under sea-level rise has not been previously assessed.

3. Methods

3.1 Model components and scenario selection

In order to simulate the ecogeomorphologic processes and feedbacks during wetland evolution we adapt the modelling framework developed by Rodríguez et al. (2017) to study wetland resilience to sea-level rise. The framework includes several individual models that operate at different time scales, which are compatible with the dynamics of the different processes simulated (Saco and Rodríguez, 2013). We use a spatially distributed hydrodynamic model with a high temporal resolution to predict the wetting and drying regime of the entire wetland during tides, from which we extract yearly measures (prevailing conditions) to drive a vegetation model that includes mangrove, saltmarsh and unvegetated substrates. Vegetation characteristics and distribution together with hydrodynamic conditions are coupled to a geomorphological evolution model to update the landscape topography every 20 years. The updated topography and vegetation distribution are incorporated into the hydrodynamic model to include feedbacks through updated hydraulic resistance values and updated soil surface elevations at every point in the wetland. Also at this time step, water

levels at the wetland entrance are updated to account for sea-level rise effects. The 20-year time step is a compromise between computational time and process description and is compatible with the slow dynamics of the system, both in terms of sea-level rise and geomorphological evolution. This type of simplifications in the temporal description of some of the processes are common in long-term wetland evolution studies (Kirwan et al., 2010; D'Alpaos et al., 2007; Kirwan and Murray, 2007; Fagherazzi et al., 2012).

The distribution of wetland vegetation is determined by first calculating the prevailing spatially distributed hydraulic conditions over a year of tidal inflows, and then applying vegetation establishment rules based on watering preferences of mangrove and saltmarsh. We integrate values of spring depth below mean high tide *D* and spring-tide hydroperiod *H* from hydrodynamic simulations in order to account for attenuation effects within the wetland. Spring-tide hydroperiod refers to the ratio between the time inundated during spring tides and the duration of all spring tides in the year. This approach deviates from "bathtub" models (Kirwan and Murray, 2007, Lovelock et al., 2015) where no attenuation is considered and also from other models that do consider tidal attenuations, but have not specifically analysed the potential effects it has on vegetation (D'Alpaos et al., 2006, Tambroni and Seminara, 2012, Temmerman et al., 2005, Temmerman et al., 2012, but see Mudd et al., 2004).

The modelling framework is used to simulate wetland vegetation evolution under sea-level rise for three different control scenarios at the inlet. The first scenario considers unrestricted tidal inflows at the wetland entrance and represents a baseline for comparison. A gate for hydraulic control at the Fish Fry Creek inlet can reduce mangrove population and prevent encroachment on saltmarsh (Rodríguez and Howe, 2013, Howe et al., 2010). The gate is modelled as a weir, and two different positions of the gate level are considered in the other two scenarios. A fixed gate scenario with a level of 0.35 m Australian Height Datum (mAHD) that has been proposed to control mangroves under the present conditions, and a rising gate scenario with the gate level starting at 0.35 mAHD and gradually rising following the rising sea-level. Previous simulations (Howe, 2008) have shown that Wader Creek inlet conveys approximately only 1% of the tidal flow exchange between Area E and the Hunter Estuary; therefore, inlet conditions in Wader Creek were not changed in any scenario.

3.2 Hydrodynamic model

Model setup

Tidal flows are modelled with a quasi-2D hydrodynamic model, developed for describing wetting and drying processes in floodplain systems (Riccardi, 2000). The model structure is based on the interconnected cells scheme originally proposed by (Cunge, 1975) and uses simplified versions of the shallow water equations as required. Full dynamic equations are used for channel flow, but for slow floodplain flow, in which inertial effects can be neglected, a diffusive wave simplification is used (Neal et al., 2012). Other simplifications are used for culverts and weirs. The model domain is discretised into a 10 m resolution squared grid, resulting in a total of 13543 cells. Shallow water equations are then solved with a two-dimensional finite differences scheme. Boundary conditions at the entrance (Fish Fry Creek and Wader Creek inlets) consist of water surface elevations in the Hunter Estuary.

At each time step, the hydrodynamic model first solves mass conservation to provide water surface elevations:

$$S_i \frac{\mathrm{d}z_i}{dt} = \sum_{k=1}^{j} Q_{k,i} \qquad [1]$$

where S_i and z_i are surface area and water surface elevation at cell i, respectively. Cells can either represent the channel network or the floodplain, so the link between cells depends on the type of cell. They can also be connected by a culvert or weir-type link. Equations describing the discharge $Q_{k,i}$ between cell i and its k=1 to j neighbouring elements are based on the momentum conservation or energy equation according to the type of link and are computed from the water surface gradient (z_k - z_i). For example, a floodplain link uses a diffusion wave approximation that considers gravity, hydrostatic pressure, and friction forces, but neglects inertial terms in the conservation of momentum equation. For (z_k - z_i) > 0, the resulting discharge equation from cell k into cell i has the form:

$$Q_{k,i} = \frac{A_{k,i} {R_{k,i}}^{2/3}}{n_{k,i}} \left(\frac{z_k - z_i}{x_k - x_i}\right)^{1/2} \qquad [2]$$

where $A_{k,i}$, $R_{k,i}$, and $n_{k,i}$ are respectively the cross-sectional values of the area, hydraulic radius and Manning roughness computed as an average of the values at cells k and i.

In the case of flow over obstacles like roads and embankments, the model uses the following broad crest weir relationships derived from the energy equation between the upstream cell *k* and cell *i*:

$$Q_{k,i} = C_{d1} \cdot b \cdot \sqrt{2g} \cdot (z_k - z_w)^{3/2} \quad \text{if } z_i\text{-}z_w < 2/3(z_k\text{-}z_w)$$
$$Q_{k,i} = C_{d2} \cdot b \cdot \sqrt{2g} \cdot (z_i - z_w)\sqrt{z_k - z_i} \quad \text{if } z_i\text{-}z_w \geq 2/3(z_k\text{-}z_w) \qquad [3]$$

which account for free and drowned discharge conditions, respectively. In the previous equations, z_w is the weir elevation, b is the width of the weir and C_{d1} and C_{d2} are discharge coefficients for free and drowned discharge conditions. Based on previous research (Cunge, 1975) and our own experience (Riccardi, 2000) we use constant standard values of C_{d1}=0.3 and C_{d2}=0.8.

Culverts are considered broad crested weirs when they flow under gravitational influences only. When surcharge conditions occur at the entrance the following culvert equations, also derived from energy principles, are used:

$$Q_{k,i} = \sqrt{2g}\left(\frac{z_k - z_{critical}}{\frac{1}{C_{d1}^2 A_c^2} - \frac{1}{A_k^2}}\right)^{1/2} \quad \text{if } z_i < z_{critical}$$
$$Q_{k,i} = \sqrt{2g}\left(\frac{z_k - z_i}{\frac{1}{C_{d2}^2 A_c^2} - \frac{1}{A_k^2}}\right)^{1/2} \quad \text{if } z_i > z_{critical} \qquad [4]$$

accounting for free and drowned discharge conditions, repectively. In the equations, A_k is the cross sectional area at the entrance, $z_{critical}$ is the critical depth at the culvert outlet and A_c is the corresponding wetted cross-sectional area.

The system of equations is numerically solved using a Gauss-Seidel iteration method and the Courant-Friedrichs-Lewy celerity condition is used for stability of the model. Channel cells are assigned a trapezoidal cross section in the direction of the flow. Floodplain cells incorporate sub-grid relief variability by defining small trapezoidal channels in the two possible flow directions draining to the cell centre, as typically done in this type of models to account for initial water storage before the filling up process (Neal et al., 2012, Stenta et al., 2017, Yamazaki et al., 2011). The channels are only 0.01 m deep and prevent the model to

compute very small depths and unrealistically high velocities during the wetting and drying process. When tracking the wet-dry front, cells with water depths below 0.01 m are considered dry cells.

Model calibration and model testing

During 2004 , water depths were measured every 15 min using pressure transducers (Solinst MLT 3001 to ± 5 mm) at three different locations in the study site: TBG, WPW and Bridge (Table 1 and Fig. 1). From this record we selected three time series of 97 hours each, one for model calibration and two for model testing. Measurements at the Bridge location were used to define the inlet boundary condition as it is located at Fish Fry Creek inlet. The same boundary condition was used at the other inlet in Wader Creek, under the assumption of no changes in the water surface elevations along the river over such a short distance. The records at the other two locations were used for calibration and testing of the model.

Table 1. Model performance for 3 water depth time series used in calibration and model testing.

Series and location		**RSR**	**PBIAS (%)**	**NS**
S1 Calibration (15/09/2004) – (19/09/2004)	TGB	0.03 (Excellent)	-0.29 (Excellent)	0.99 (Excellent)
	WPW	0.04 (Excellent)	3.68 (Excellent)	0.99 (Excellent)
S2 model testing (27/09/2004) – (01/10/2004)	TGB	0.06 (Excellent)	-1.69 (Excellent)	0.99 (Excellent)
	WPW	0.05 (Excellent)	6.04 (Excellent)	0.99 (Excellent)
S3 model testing (13/10/2004) – (17/09/2004)	TGB	0.08 (Excellent)	-6.96 (Excellent)	0.99 (Excellent)
	WPW	0.07 (Excellent)	2.27 (Excellent)	0.99 (Excellent)

In order to evaluate the performance of the model, we used statistical indicators commonly used in hydrological models (Moriasi et al., 2007): the ratio of the root mean square error to the standard deviation of measured data (RSR), the Nash-Sutcliffe efficiency (NSE), and the

per cent bias (PBIAS). Performance is considered excellent when: RSR < 0.50, -10% < PBIAS < 10% and NSE > 0.75 (Moriasi et al., 2007). Performance values are presented in Table 1. Model testing values show an excellent performance of the model in locations TGB and WPW, with performance indicators values at the same level or better than values previously reported for similar models (Temmerman et al., 2005, Carniello et al., 2011). Comparison plots of simulated water level are presented in the Supplementary Material (Supp. Figs 3-5).

The calibration of the model consisted in obtaining the best performance of the model by using Manning's roughness *n* as the calibration parameter. A set of combinations of values of *n* based on measured data was tested for each vegetation coverage represented in the model. The measured values of flow resistance were obtained by measuring water surface slopes with a Sokkia SDL30 automatic level sensor (to ±1mm) and velocity with acoustic Doppler velocimetry (ADV) (to ± 2.5 mm s^{-1}) both in the field and laboratory (Howe, 2008; Rodríguez and Howe, 2013). Table 2 shows the range of values testes for each area and the final values obtained after calibration. Roughness values similar to the range tested during calibration have been reported for estuarine environments (Dietrich et al., 2011, Mazda et al., 1997).

Table 2. Calibrated values of Manning's *n* roughness.

Soil coverage	**Range tested**	**Final calibrated values**
Unvegetated	0.08 - 0.15	0.12
Mangrove	0.1 - 0.7	0.50
Saltmarsh	0.1 - 0.5	0.15
Channels	0.03 - 0.04	0.035

Note: Manning's *n* units are $s/m^{1/3}$

3.3 Vegetation model

Model setup

Coastal vegetation responses to tidal flows can be modelled using time-aggregated variables that are computed from inundation time and water depth. Vegetation establishment rules were introduced in our model defining suitable ranges on two variables often used to describe the response of estuarine plant species: the depth below mean high tide D (in m) and the ratio of inundated time over total time, usually referred to as hydroperiod H (dimensionless) (Kirwan et al., 2010, D'Alpaos et al., 2007, Kirwan and Murray, 2007). Values of D and H were obtained integrating spring tide results from one year of continuous hydrodynamic simulations. During spring tides, water levels and inundation extent are more pronounced and become critical for vegetation survival (Howe, 2008).

Mangrove species require pneumatophores to be above water a minimum period of time in order to obtain enough oxygen. Soils regularly inundated, such as in estuarine environments, can experience an accumulation of phytotoxins or undergo conditions of limited oxygen availability for root uptake (Crase et al., 2013). Mangrove is considered to be sensitive to spring-tide hydroperiod, and we adopt a suitable range $0.1 < H < 0.5$ based on our *A. marina* data (Rodriguez et al., 2017; Howe et al., 2010) but also consistent with data from Crase et al. (2013). Also, mangrove propagule establishment can be restricted by high soil salinity conditions that will occur under very low values of D (Saintilan et al., 2009), so we impose an additional restriction of $D > 0.2$ m for mangrove suitable conditions.

The typical height of saltmarsh species at the site is around 25 cm; therefore, a limit of $D <$ 0.25 m was set for saltmarsh suitability conditions. We considered that D values higher than 0.25 m will drown saltmarsh and result in hypoxia, restricting their establishment (Morris et al., 2002). A limit for hydroperiod was also included in order to represent the inability of saltmarsh to colonise areas almost permanently inundated during spring tide ($0 < H < 0.8$). Finally, saltmarsh was assumed to be outcompeted by mangrove in wetland areas with adequate conditions for both species, as reported in previous work (Saintilan et al., 2014).

Model testing

In order to test our vegetation model, we compared our simulated vegetation distribution against an estuarine habitat distribution map. This map was obtained by combining RTK GPS and ground-truthed high-resolution aerial photography for the year 2007 (Howe, 2008). A long- term water level series (12 months) at a nearby gauging station from 2007 was selected

as input for our model because it was considered representative of the conditions experienced by vegetation and also because it was one of the few long terms records without missing data. Initial observed vegetation distribution was used for set-up of the model roughness. As shown in Fig. 2, model simulations agree remarkably well with observations. The model predicted values of percentage wetland area with mangrove and saltmarsh of 9% and 49%, respectively. These values compared favourably with mangrove and saltmarsh measurement of 8% and 39%, respectively. We also computed the accuracy and the true positive rate of our predictions by identifying the proportion of our simulated vegetated area that spatially coincided with the estuarine habitat map. The model presented a very good accuracy of 0.95 and 0.73 for mangrove and saltmarsh, respectively. True positive rate values also show a good prediction of mangrove and saltmarsh with values of 0.69 and 0.78. A general confusion matrix is presented in the Supplementary Material (Supp. Table 1).

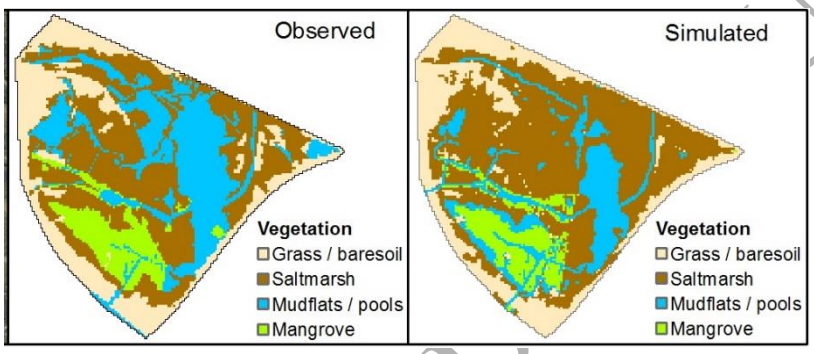

Figure 2. 2007 vegetation distribution on Area E: a) observed , b) simulated (modified from Rodríguez et al. (2017)).

3.4 Ecogeomorphic evolution model

Model setup

In order to include changes in soil surface elevation for long-term projections of sea level rise (Fagherazzi et al., 2012, Kirwan and Megonigal, 2013), we adapt a previous methodology ("Kirwan model") based on saltmarshes in the US (Kirwan et al., 2010). The model calculates a variable surface elevation rate (*dE/dt*) at each point in the wetland by including the contribution of biomass and suspended sediment deposition to the accretion process.

$$\frac{dE}{dt} = C\ (q + kB)D \qquad [5]$$

where the term *E* stands for surface elevation, *C* stands for suspended sediment concentration, *B* is the aboveground biomass and *q* is a depositional parameter. The rate at which sediment settles is represented by the parameter *q*, therefore, this parameter does not depend on vegetation. On the other hand, the term *k* represents the efficiency of vegetation to trap sediment as well as changes in elevation from organic matter accumulation. The model does not consider erosion, as it assumes that flow within the wetland is too slow. Aboveground biomass *B* increases with *D* until it reaches an optimum value, beyond which biomass decreases. The relation proposed by Morris et al. (2002) for saltmarsh biomass was used in this study:

$$B = aD + bD^2 + c \qquad [6]$$

where the parameters *a*, *b* and *c* are coefficients that need to be determined empirically.

The value of suspended sediment concentration *C* in equation [5] is spatially variable in our formulation. *C* is higher close to tidal channels and the wetland entrance, as shown by previous research (D'Alpaos et al., 2007, Kirwan and Guntenspergen, 2010, Kirwan and Murray, 2008) and data collected at the site (Howe, 2008). When plotting our sediment concentration data (Howe, 2008) against distance to inlet we observed the same exponential decay trend with distance that Kirwan and Guntenspergen (2010) and Kirwan and Murray (2008) used to describe spatially variable *C* in their models (Supp. Fig. 6a), although not as strong. Our values of *C* also decreased linearly with decreasing measured values of *D* (Supp. Fig. 6b), with this linear relation (r^2=0.74) providing a slightly better predictive capacity than the exponential decay (r^2=0.68). Because of the complex flow paths within the wetland implementing a model based on distance to the inlet of all 13546 cells was impractical, so the empirical relationship between *C* and *D* was used to consider a variable sediment concentration in the model. Sediment concentration values at the site are described as:

$$\frac{C}{C_{max}} = 0.55\ D + 0.32 \qquad [7]$$

where C_{max} = 37 g/m^3 is the maximum concentration value at the wetland inlet. It must be pointed out that our simple empirical sediment concentration distribution, while reasonably

representing the conditions in our wetland, is empirical and as such must be used with caution in other systems.

Erosion is not considered in the model, as it is assumed that in general vegetation stabilises sediment and prevents erosion at tidal pool margins. Fluvial erosion has not been identified as an important processes in the study site for long-term simulations as the stream network has remained stable for many years (Howe, 2008) and episodic storm events have shown reworking of sediments in the vegetated areas rather than net erosion (Rogers et al., 2013). Erosion by wind waves is limited by the small size of permanent pools and wind-break effects of infrastructure under current conditions (Howe, 2008), but may become more important as sea-level rises and permanent pools increase their size (Carniello et al., 2011; Leonardi et al., 2016). However, it is likely that wetland submergence due to the limited accretion capacity of our attenuated system will still be the dominant mechanism of wetland loss during sea-level rise, similarly to Ravens et al., (2009).

Model calibration

The calibration of our soil surface elevation model consisted in obtaining the parameters that produced the best match of the results of equation [5] with local data. Our local data consisted of a 10-year record (2002-2012) of surface elevation changes derived from Surface Elevation Tables (SET) (to ± 1.4 mm) (Rogers et al., 2013). This record provided estimates of 2.23 mm/yr and 1.39 mm/yr increases in soil surface elevation for mangrove and saltmarsh, respectively. We also adopted a value of q of 0.0009 m^3/yr, which is the same value reported for *Spartina alterniflora* saltmarshes in South Carolina, US (Kirwan et al., 2010, Morris et al., 2002).

In order to obtain site-specific values of k for saltmarsh and mangrove, we use average values of D, B and C. Average D values were obtained by running the hydrodynamic model for a year and averaging all local D values over the corresponding vegetation. Average C values were calculated from gravimetric analysis collected on site (Howe, 2008). Average values of D and C are presented in Table 4. In the absence of local biomass values, values from a neighbour site with similar vegetation characteristics were used (Kelleway et al., 2016). Final calibrated values for k are consistent with reported values for saltmarshes in South Carolina (Table 4). The value of k associated with mangrove vegetation is lower because only a small part of the tree is submerged and not all biomass contributes to sediment entrapment.

The biomass coefficients are determined following the same rationale than Morris et al. (2002) for US saltmarshes. The parameters of the biomass curve described by equation [6] can be adjusted so that the average value of *D* corresponds to the average value of biomass for our site (Table 4) and at the same time a value of D = 0.25 m produces the maximum biomass. Further increases in *D* results in biomass decrease (saltmarsh die-off) due to hypoxia, which agrees with our vegetation model based on the characteristics of the saltmarsh in our site.

As done in previous research for other vegetation species (D'Alpaos et al., 2007), we adapt the equation for saltmarsh to model mangrove biomass. The coefficients *a*, *b* and *c* are obtained to capture mangrove suitability conditions, that is, *D* less than 0.2 m is too shallow and saline for mangrove colonization and *D* above 1.1 m is associated with undesirable inundation conditions. As in the saltmarsh case, the average value of *D* for mangrove results in the average value of mangrove biomass reported in Table 4.

Table 4. Parameters for soil surface elevation model.

Model parameters	**South Carolina Saltmarsh** (Kirwan et al., 2010, Morris et al., 2002)	**Area E Saltmarsh**	**Area E Mangrove**
Average D (m)		0.142	0.474
Average C (g/m^3)	20	15	22
Average B (g/m^2)		900	1000
k (m^5/g^2)	7.5×10^{-7}	6.2×10^{-7}	1.2×10^{-7}
Maximum B (g/m^2)	1868	1050	1223
a (g/m^3)	15500	8384	7848.88
b (g/m^4)	-18550	-16767	-6037.6
c (g/m^2)	-1364	0	-1328.27

3.5 Sea level rise projections

For long term simulations, we considered an accelerated rate of sea-level rise over the next 100 year following the RCP8.5 scenario (Church et al., 2013), according to which rates of

sea-level rise increase from 4 mm/yr up to 11 mm/yr. The initial rate was corroborated with data from a gauging station located upstream of the wetland site (Hexham bridge). The same data does not show any changes in the amplitude of the tide over the last 10 years, so we did not considered amplitude changes over time. Also, we did not consider any tide modulation effects of the estuary as sea-level rise values similar to those in the estuary were reported for a nearby ocean tide station (Rogers et al., 2013).

4. Results

Model predictions of spatial vegetation changes over 100 years of sea level rise under different inlet control scenarios are shown in Fig. 3. As previously explained initial conditions for these simulations correspond to Fig. 2b, and successive changes in vegetation, accretion and sea level are incorporated into the hydrodynamic model every 20 years. Vegetation changes observed in Fig. 3 have been summarized in Fig. 4 in terms of percentage area cover corresponding to mangrove, saltmarsh and mudflat/pools. As seen in these figures the evolution of vegetation significantly differs for the various inlet control scenarios simulated (i.e., no control, fixed gate and rising gate) as discussed below.

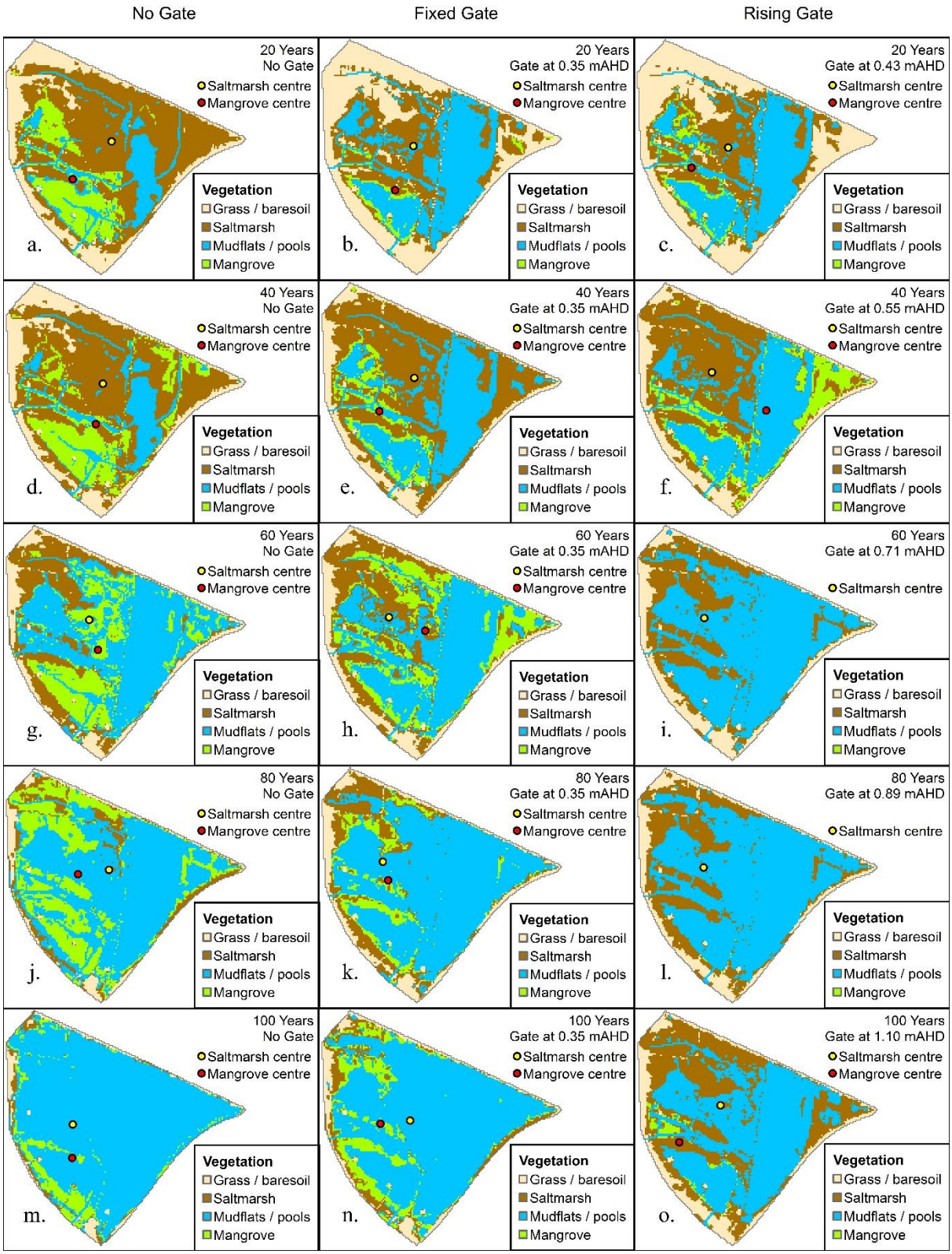

Figure 3. Simulated vegetation evolution from 20 to 100 years under: a,d,g,j,m) uncontrolled scenario (modified from Rodriguez et al., 2017), b,e,h,k,n) fixed gate scenario and c,f,i,l,o), rising gate scenario.

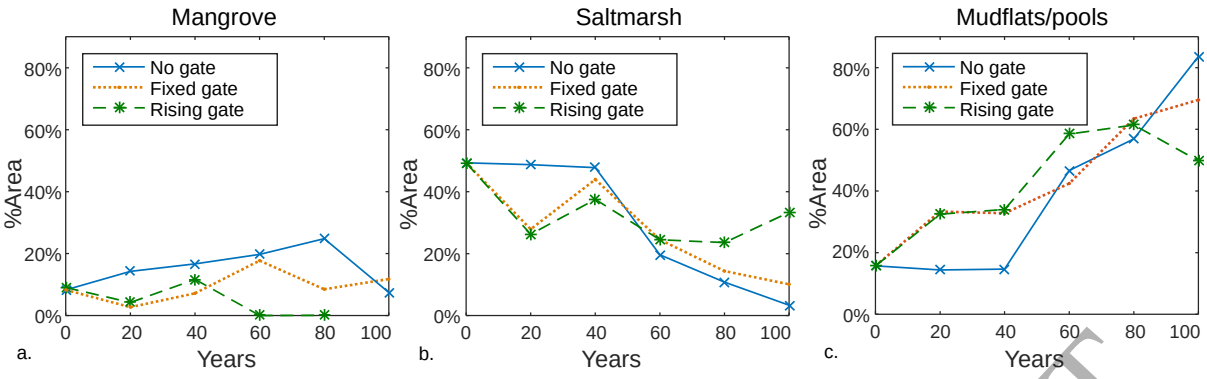

Figure 4. Percentage area cover under different inlet control conditions: a) mangrove, b) saltmarsh, c) mudflat and tidal pool.

The model predicts relatively small changes in vegetation dynamics during the first 40 years, of low sea-level rise values, under uncontrolled conditions (Fig. 3a,d). Mangrove vegetation in Fish Fry Creek persists because the hydroperiods in this area remain relatively unchanged at values below 0.5 (Supp. Fig. 7). Mangrove colonization of the upper wetland areas in Wader Pond and Swan Pond is also observed and is induced by the effect of improved recruitment conditions in these areas. Although saltmarsh is displaced by mangrove encroachment, the total reduction in saltmarsh area is small (Fig. 4b) as it is compensated by colonization of higher areas in the tidal frame that, as sea level rises, achieve more suitable inundation conditions for saltmarsh. Little change is predicted for mudflat and tidal pool areas. At 60 years, saltmarsh submergence due to a higher rate of sea-level rise (8 mm/year) is observed (Fig. 3g). Mangrove areas in Fish Fry Creek are still able to survive, partly due to high accretion values in these areas (more details in the discussion). Wader Pond and Swan Pond areas that were invaded by mangrove at 40 years are predicted to disappear, but migration into higher ground induced by sea-level rise produces further encroachment on saltmarsh (Fig. 3g). Submergence of saltmarsh and mangrove encroachment into saltmarsh areas leads to a significant simulated saltmarsh loss. Saltmarsh percentage area reduces from 50% at 40 years to only 20% at 60 years (Fig. 4b). Simulations for 80 years, under a sea-level rise rate of 9 mm/year, suggest that conditions in the upper tidal frame will be favourable for mangrove colonization. Mangrove cover increases by displacing saltmarsh, whose extent is further reduced to 10% of the wetland area (Fig. 3j and Fig. 4a, b). Finally, predictions for 100 years with sea level rising at a rate of 11 mm/year show that hydrodynamic conditions become unfavourable for both mangrove and saltmarsh survival (Fig. 3m). As much as 85% of the wetland area is covered by tidal pools and mudflats (Fig. 4c), including most of the

original mangrove areas in Fish Fry Creek. Only a small area of mangrove vegetation remains in a region of high elevations near the inlet and saltmarsh is practically absent.

The second set of simulations (second column in Fig. 3) corresponds to the introduction of a control gate at a fixed height of 0.35 mAHD at the Fish Fry Creek inlet. Our results show that after 20 years the change in hydrodynamic conditions induced by the hydraulic control produces ponding behind the gate, which increases hydroperiods (Supp. Fig. 8) and eliminates most of the initial mangrove vegetation on both Fish Fry Creek and Wader Creek (Fig. 3b). In this scenario, saltmarsh areas are not reduced due to mangrove encroachment as observed in the case with no gate. However, tidal flow attenuation from the gate reduces the extent of inundation of areas in the upper tidal frame, therefore reducing saltmarsh areas from 40% to 30% of the wetland area. Another interesting result from the simulation is the increase in mudflat and tidal pool areas of Swan Pond, as a result of the propagation of semi-stagnant conditions on Fish Fry Creek into the inner compartments. After 40 years, sea-level rise promotes a recovery of saltmarsh vegetation on the upper tidal frame (Fig. 3.e). Mangrove vegetation encroachment into saltmarsh areas is observed on the upper attenuated compartments. Predictions for 60 years reveal further invasion of mangrove vegetation reaching areas that are at higher elevation than those invaded in the uncontrolled condition scenario (Fig. 3.h). Simulated mudflat and tidal pools areas are smaller than those for the uncontrolled scenario because the gate attenuation effects induce a general decrease in *D* but an increase in hydroperiod in the upper compartments of the wetland (Supp. Fig. 8g,h). These conditions are favourable for mangrove encroachment that continues to increase, but also enables the survival of saltmarsh in the upper areas. As a result, the % coverage of mudflat and tidal pool areas is smaller than in the no inlet control case. Predictions for 80 years show a substantial decline in both mangroves and saltmarsh (Fig. 3k). At the end of the simulation period few peripheral areas of mangrove and saltmarsh remain, with mudflat and tidal pool areas occupying most of the wetland.

Predictions for the rising gate scenario after 20 years show very similar vegetation patterns to those of the fixed gate at 0.35 mAHD (Fig. 3b,c and Fig. 4), even though the gate height is at 0.43 mAHD. Further increase of the gate height to 0.55 mAHD at 40 years produces a general increase in water depths on Swan Pond, which promote the invasion of mangroves (Fig. 3f). The most notable change in the wetlands dynamics for this scenario is predicted at 60 years when the height of the gate is increased to 0.71 mAHD. High hydroperiods are

predicted in most of the wetland, but shallow water depths are maintained on the upper tidal range (Supp. Fig. 9g,h) which promote saltmarsh establishment and exclude mangrove vegetation from the entire wetland. Simulations at 80 years and 100 years (Fig. 3 l,o) produce similar results with a slight increase of saltmarsh vegetation at 100 years.

The magnitude of changes in wetland coverage can be better appreciated by calculating the changes of the ratio of vegetated to non-vegetated areas (mudflats/pools) from the data of Fig. 4. Initial ratios of 70% (mangrove/non-vegetated) and 30% (saltmarsh/non-vegetated) are reduced to only 10% for both vegetation types over the period of simulations for the scenarios without gate and with fixed gate. The scenario with the raising gate shows a significant difference with the previous two scenarios with no remaining mangrove, but a much larger value of the final saltmarsh to non-vegetated ratio (70%).

The results of Fig. 3 show important migration of the vegetation communities during sea-level rise. In order to quantify this migration, the position of each vegetation community (mangrove and saltmarsh) at each time step has been included in the figure by plotting the centroid of all areas occupied by the respective vegetation. Tracking the position of the centroids over time gives an estimate of the migration of the vegetation as presented in Fig. 5. The figure shows that mangrove migration is larger and faster than saltmarsh migration, which reflects the fact that mangrove actively colonises the northern areas of the wetland. Saltmarsh has less capability to migrate as it is already in the areas with higher topography. Migration towards areas with suitable conditions occurs mostly North for mangroves while saltmarsh migrates predominantly towards the West (Fig. 3), with clear migration limits of 400 m in mangrove and 250 m in saltmarsh due to the presence of the outer embankment. When these limits are reached, vegetation coverage is substantially reduced (Fig. 4) and restricted to peripheral areas. As seen in Fig. 5, the migration rates are higher for the scenarios with the gate at the inlet, particularly for the case with the rising gate. As we will discuss further in the next section this migration rates are influenced by hydrodynamic conditions and geomorphic feedbacks that provide mechanisms for the vegetation to adapt to changing sea levels.

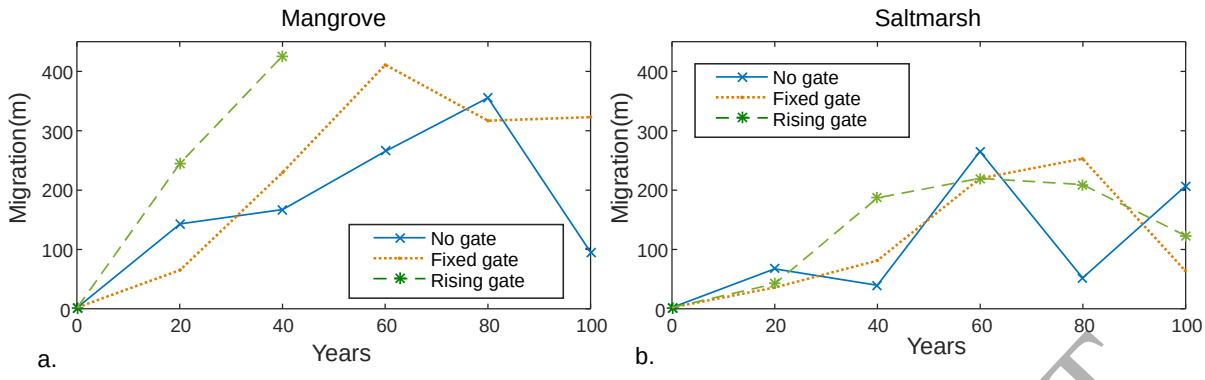

Figure 5. Vegetation migration under different inlet control conditions: a) mangrove, b) saltmarsh

When attenuation effects are not considered water surface elevations within the wetland are the same as in the estuary, and any changes in sea-level are directly propagated into the wetland. In our study site the inundation regime is heavily attenuated by the presence of inlet and internal controls, and our hydrodynamic model results show marked difference between the water levels in the estuary and inside the wetland. For example, Fig. 6 shows how attenuation modifies mean high water (MHW) levels in the wetland areas occupied by mangrove and saltmarsh as sea-level rises. MHW values over mangrove and saltmarsh have been obtained by spatially averaging the local values of MHW over all mangrove and saltmarsh cells in each time step, respectively, and are compared against the values in the estuary. Both mangrove and saltmarsh experience lower MHW than the estuary MHW because of highly attenuated conditions inside the wetland due to inlet conditions and internal earthworks, levees and culverts. This attenuated regime drives the evolution of the wetland as it controls not only vegetation establishment and survival but also the capacity of vegetation to adjust vertically via accretion (equation 5). There is also a clear trend of lower MHW when the gate restricts the flow to the wetland compared to the unrestricted inlet situation.

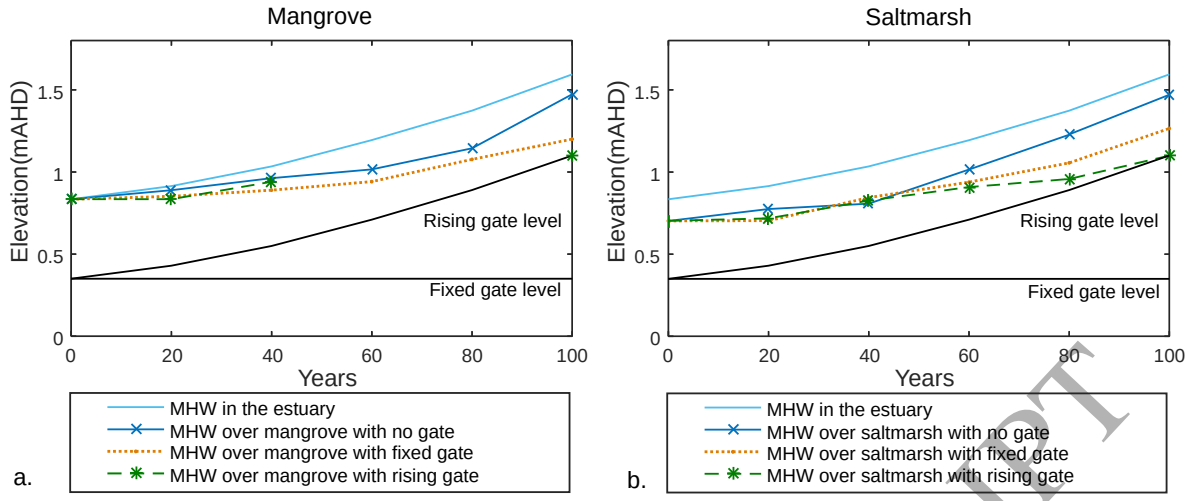

Figure 6. Mean high water (MHW) levels in the estuary at the wetland entrance and average MHW levels over vegetation inside the wetland under different inlet control conditions: a) mangrove, b) saltmarsh. The heights of the gates for both control scenarios have also been included as a reference

4 Discussion

Our long-term simulations show that the wetland is not in equilibrium as it is continuously adapting to sea-level rise due to an important elevation deficit. Particularly for the no control and fixed control scenario, the wetland almost completely disappears after 100 years of sea-level rise. This time to submergence is broadly consistent with the values of D'Alpaos et al., (2011) for microtidal saltmarshes under comparable sea-level rise and sediment characteristics. Even though our estuary can be classified as mesotidal, internal attenuation in most areas of our wetland produces flow conditions that are more consistent with a microtidal environment. Rising the gate following sea-level rise delays this total submergence.

Besides predicting wetland evolution under sea-level rise and human interventions, our simulations allow us to the study the different mechanisms involved in vegetation establishment and survival. Vegetation resilience and persistence during sea-level rise is highly dependent on its vertical adjustment capacity, which is a mechanism of elevation gain through accretion (Lovelock et al., 2015). However, accretion rates that can potentially counteract submergence primarily occur in areas with high sediment supply (Kirwan and Megonigal, 2013, Kirwan et al., 2016, Rodríguez et al., 2017, though see McKee et al., 2007). Another important mechanism for vegetation survival is inland migration, in which

vegetation colonizes higher areas in the tidal frame and therefore gains elevation by spatial adjustment. However, this spatial adjustment is limited by the possibility of accessing higher topographic areas with adequate hydrodynamic conditions (*D* and Hydroperiod) (Woodroffe et al., 2016, Morris et al., 2002), which is sometimes not possible due to urbanization or alternative land uses. In Area E, levees surrounding the wetland limit wetland migrations landwards. Both elevation gain mechanisms (vertical adjustment due to accretion and spatial adjustment enabled by migration) occur in each of the scenarios analysed but to a varying degree.

Attenuated flow conditions reduce local *D* values (Supp. Fig. 7) and therefore accretion rates (equation 5). Even though accretion rates are notably restricted by attenuation (Fig. 6), vegetation is still, to some extent, able to survive sea-level rise by moving to higher wetland areas with more suitable inundation conditions (Figs. 3 and 4). For the uncontrolled inlet scenario mangrove gradually invades saltmarsh areas during sea-level rise. The mangrove core at Fish Fry Creek is able to withstand sea-level rise for most of the simulation period, with emerging mangrove patches appearing in all other compartments. This colonization is regulated by hydroperiod conditions, but emerging mangrove patches are less persistent and less resilient to sea-level rise presenting patterns of active die-off and recolonization. The new patches of mangrove appear further to the north where *D* values are typically low (Supp. Fig. 7). Low values of *D* are associated with low biomass (equation 6) and low sediment concentration (equation 7) which is consistent with the fact that the emerging mangrove growth is limited by shallow water conditions and are located farther away from the inlet so receive less sediment. Soil accretion in these areas is therefore not enough to produce vertical adjustments similar to the ones at Fish Fry Creek and necessary for survival. As a result, mangrove spatial adjustment by encroachment on saltmarsh with suitable hydroperiod conditions, is the only mechanism that allows its survival. The resilience of the Fish Fry creek mangrove core results in a tendency of the centroid to remain close to the wetland entrance, slowing down the overall migration (Fig 5a). While mangrove migrates inland encroaching on saltmarsh (mostly north), saltmarsh migration to further northern locations is prevented by the close proximity of a levee (Fig. 1). Initially saltmarsh colonises higher topography on the west part of the wetland but at a slower pace than mangrove (Fig 5b). Eventually mangrove overtakes saltmarsh, which virtually disappears after 80 years (Figs. 3 and 4b). Most studies of Australia coastal wetlands show this trend of mangrove encroachment on saltmarsh (Ward et al., 2016 and references therein).

Spatial adjustment becomes more important for mangrove survival under conditions with inlet control. The gate prevents drainage of the wetland via Fish Fry Creek inlet which leads to longer inundation time and therefore increased hydroperiod. In the scenario with the fixed gate at 0.35 mAHD, the mangrove area at Fish Fry Creek is immediately affected by increased hydroperiods beyond the acceptable value of 0.5. With hydraulic control, mangrove area is reduced to half of the initial vegetation and reaches a minimum extension after 20 years (Fig. 4a). After this initial period, spatial adjustment drives mangrove to encroach on saltmarsh in areas with suitable hydroperiod and depth. In common with the uncontrolled scenario, vertical adjustment in the emerging mangrove is not enough to promote persistence, which leads to die-off and colonization of new areas. Because of the absence of the mangrove core at Fish Fry Creek, the centroid of mangrove areas progresses north more rapidly than in the uncontrolled conditions (Fig. 5a). Introduction of the gate produced also an initial decrease of saltmarsh extension in the higher (north-west) areas of the wetland because of the flow attenuation, which was rapidly recolonised with increasing sea level (Fig.3 and 4b). A very similar pattern of saltmarsh migration and mangrove encroachment on saltmarsh to that under uncontrolled conditions occurs with the fixed gate control. Compared to the uncontrolled condition (Fig.3) the effects of the fixed gate are mostly limited to the Fish Fry Creek mangrove core without important modifications to the vegetation evolution in the rest of the wetland. An inlet gate with a fixed level can be effective temporarily to control mangrove, but sea-level rise eventually produces conditions for mangrove encroachment.

Raising the level of the gate at the inlet in order to match the sea-level rise has a big impact on mangrove response. This scenario is as effective as the previous one in eliminating the mangrove core at Fish Fry Creek, but it also prevents colonisation of the northern areas of the wetland. Mangrove is excluded from these areas by maintaining very low values of depth (Supp. Fig. 9) that generate salinity conditions beyond the tolerance of mangrove propagules (see methods). These low values of depth are maintained relatively constant during sea-level rise so mangrove is unable to access higher areas of the wetlands and disappears completely after 40 years (Fig 3 and 4a). During this period colonization is restricted to a patch in the north east end of the wetland and far from the initial mangrove location, which explains the high migration rate of Fig. 5a. Mangrove exclusion from the northern part of the wetland benefits saltmarsh, which is able to cope with sea-level rise with only minor losses to its initial extent (Figs. 3 and 4b). Migration of saltmarsh is mostly to the west and at a similar

rate than in the previous two cases. Fig. 4c shows that the scenario with a rising gate results in less combined vegetation loss after 100 years of sea-level rise, and it therefore produces the lower final amount of non-vegetated mudflats and tidal pools.

As explained before, the total elevation gain of the vegetation results from the combined effect of vertical adjustment (through accretion) and spatial adjustment (through migration). Even though vegetation elevation gain follows the increase in water levels due to sea-level rise in all scenarios, the relative contribution of vertical versus spatial adjustment may differ because of the different vegetation dynamics. We therefore complement our previous analysis by looking at the two contributions to elevation gain. Fig. 7 includes the average soil elevation of each vegetation (as a result of the total elevation gain) obtained from the model outputs at each time step, as well as the contribution of the vertical accretion adjustment to the total soil elevation.

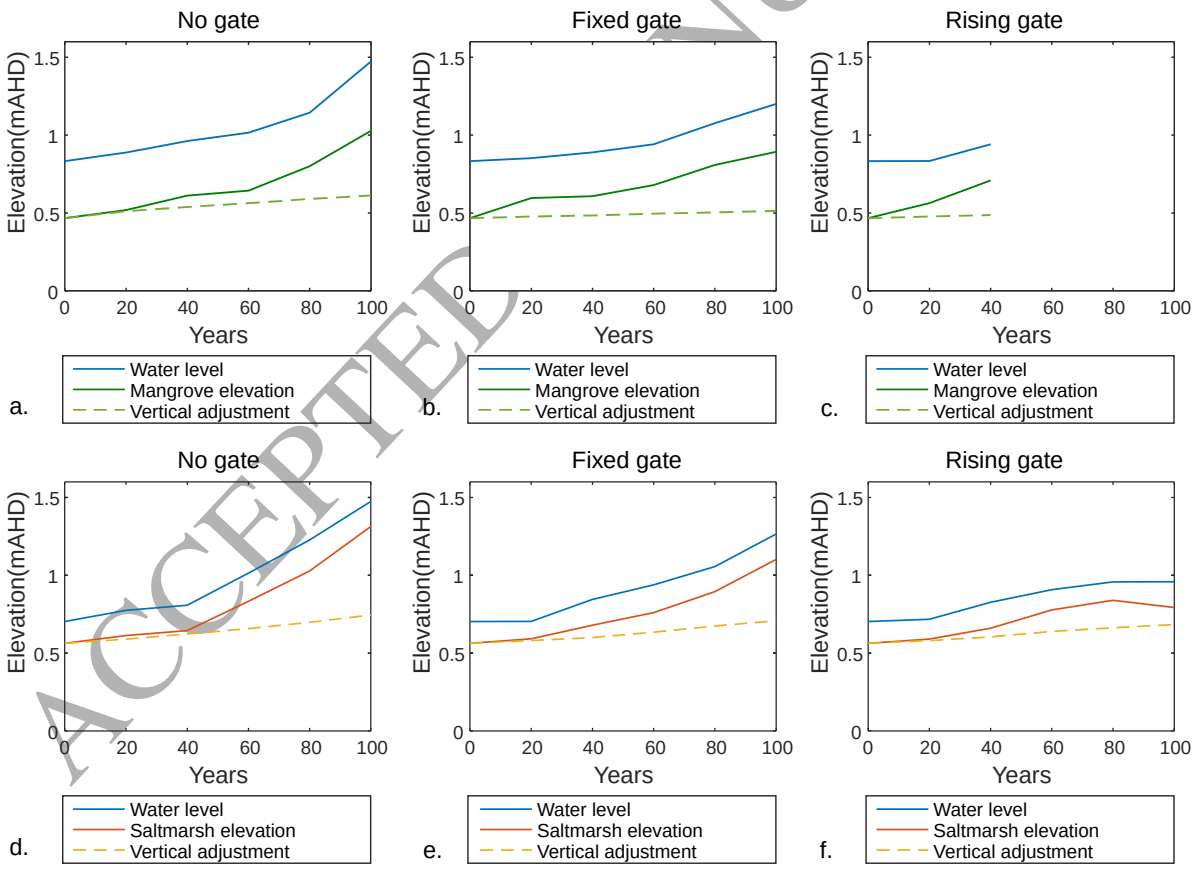

Figure 7. Spatially averaged elevations and spatially averaged contribution of vertical adjustments induced by bio-geomorphic accretion over mangroves (a,b,c) and saltmarshes (d,e,f). The spatially averaged MHW levels (blue) over mangroves and saltmarshes have also been included for comparison.

The vertical adjustment at each time step was computed by using the average value of *D* of each vegetation from the previous time step to calculate yearly accretion rates (equation 5), and integrating them over the 20-year period. This figure also displays the MHW levels over each vegetation type already presented in Fig. 6. Results in Fig. 7 confirm that for all scenarios the average vegetation elevation follows the trend of water levels inside the wetland prescribed by sea-level rise. This elevation gain is driven primarily by migration. Elevation gain by accretion is dominant only in the early stages of the simulation period, except for the case of mangrove in both scenarios with inlet gate control. In this case accretion is never dominant because mangrove is forced to migrate to areas with low values of *D* and consequently low accretion rates. In the rest of the cases, even though initial accretion is important, it rapidly becomes less than the changes in water levels due to sea-level rise. The largest accretion values occur for the uncontrolled scenario, with mangrove and saltmarsh accreting at about 2 mm/yr, at the beginning of the simulations. While saltmarsh accretion remains roughly at the same level throughout the rest of the simulations, mangrove accretion rapidly decays to less than 1 mm/yr as it colonises the attenuated compartments with higher elevation (Wader Creek, Wader Pond and Swan Pond). Compared with the uncontrolled scenario, the additional attenuation produced by the presence of the gates reduces the values of *D* and accretion for mangroves (Fig. 7a,b,c), but not for saltmarsh. Consequently, inlet gate control reduces the accretion in mangrove areas while maintaining the accretion levels in saltmarsh areas.

The contribution of migration to the total elevation gain over time is the difference between the total amounts and the accretion values shown in Fig. 7. As already pointed out this migration component depends of the areal topographic profile of the wetland under study. In order to investigate this dependence, Fig. 8 displays the migration elevation gains against the migration distance (from Fig. 5) for both mangrove and saltmarsh and for all scenarios analysed. Fig. 8 shows that all cases follow a similar trajectory with an average ratio of migration elevation gain over migration distance of 0.0005 m/m consistent with topographic

slope values specific of our wetland. However, the velocities at which these gains are achieved through migration are clearly different for the different scenarios.

Our methodology incorporates the most important processes and feedbacks that are key for the evolution of coastal wetlands under the combined influences of man-made structures and sea-level rise. However, our model has limitations that originate in simplified descriptions of model components, particularly for vegetation, sedimentation and accretion processes. These simplifications are common to most wetland evolution models, and are required in order to enable the study of relatively large systems with high resolutions over long simulation periods, which requires massive memory and computational time. For example, our suspended sediment formulation, while reasonably representing the expected behaviour in our wetland, is empirical. Therefore, as with any data-driven relation, it should be carefully tested and/or re-calibrated before using it in other systems. Previous work that has implemented more universal sediment transport formulations coupled to wetland flow models has been limited to applications in either small wetland domains (Belliard et al., 2015), short time periods (Carniello et al., 2014) or both (Temmerman et al., 2005). Future developments in computational technologies and numerical methods will allow the full use of more sophisticated and physically based methods for the solution of sediment processes over the range of scales relevant for long-term wetland management and evolution.

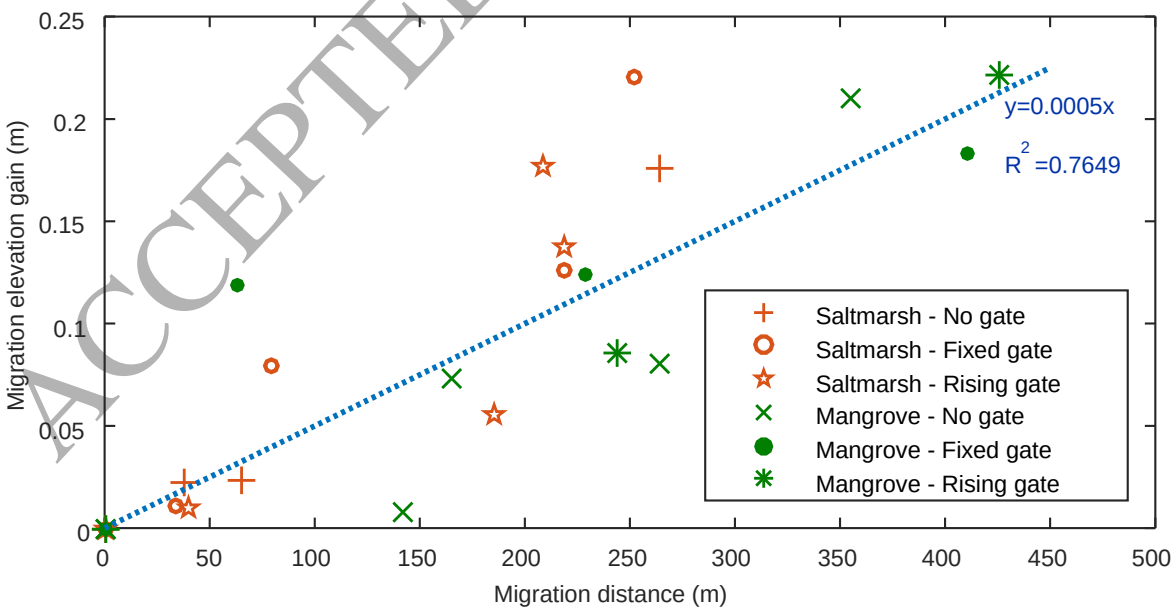

Figure 8: Elevation gain through migration of mangroves and saltmarsh for all the scenarios analysed.

5. Summary and conclusions

Accelerated sea-level rise rate is predicted to significantly reduce coastal wetland areas around the world (Kirwan and Megonigal, 2013, Lovelock et al., 2015, Craft et al., 2009). In tropical and subtropical wetlands, mangrove encroachment increases even more the vulnerability of saltmarsh (Saintilan and Rogers, 2013, Armitage et al., 2015). Mangrove encroachment can be reduced by hydraulic manipulation via inlet control, but the long-term evolution of this management alternative must be analysed together with sea-level rise.

Our study for a wetland typical of SE Australian estuaries provides valuable insight on vegetation response under heavily attenuated tidal conditions, a consequence of human interventions that are common in many areas of the world. Analysis of the response of wetland vegetation to sea-level rise in our site shows important differences among three scenarios simulated: no inlet gate control, inlet gate control at a fixed level and inlet gate control with a level rising with the sea level.

The first scenario clearly shows that without gate control mangrove will encroach on saltmarsh following the observed trend in many SE Australian estuaries. Rising sea level also results in a general increase in mudflat and tidal pool areas that displaces saltmarsh and mangrove to higher topographies. Saltmarsh disappears after 80 years, due to both encroachment by mangrove and advance of mudflats. After 100 years, all wetland vegetation is excluded because of the presence of the embankment that prevents migration.

The fixed gate control is initially very effective in excluding mangrove from the wetland while maintaining saltmarsh. However, when the MHW levels attains values above 1m by 60 years, tides are able to reach more freely the upper wetland areas and mangrove re-appear and starts encroaching on saltmarsh. After this point, the gate in no longer effective and the behaviour of the wetland vegetation is very similar to the no gate scenario, with mudflats and tidal pools occupying most of the wetland after 100 years.

Compared with the fixed gate, the rising gate has a longer lasting effect. Mangrove is rapidly excluded from the wetland and saltmarsh is maintained roughly at the same area value throughout the whole period of simulation. Rising the gate with sea-level maintains the

hydrodynamic conditions in the upper wetland areas relatively unchanged promoting saltmarsh persistence. In terms of total vegetated wetland area, this is the only scenario that is able to maintain a significant amount and partially cope with sea-level rise after 100 years.

Previous research on coastal wetlands has indicated their capacity to increase their accretion rates in response to sea-level rise, contributing to elevation gain and vegetation survival (Kirwan and Megonigal, 2013, Lovelock et al., 2015). In our study, we found that vegetation accretion rates are surprisingly low and in some cases decrease with sea-level rise. This effect is the result of a heavily attenuated tidal regime inside the wetland. Vegetation in areas with low levels of attenuation close to the entrance display high accretion rates during the initial phase of the simulations, but accretion decreases as the vegetation is displaced away from the entrance and towards the highly attenuated parts of the wetland. The low accretion rates are compensated by migration as a mechanism for elevation gain in order to cope with sea-level rise. As a general conclusion, vegetation in attenuated wetlands will display lower accretion and higher migration rates than unattenuated wetlands under similar conditions of sea-level rise and sediment supply. Attenuated conditions are likely to be present in many estuarine wetlands worldwide, as coastal areas tend to be highly urbanized.

Acknowledgments

J.R. acknowledges support from the Office of Environment and Heritage. P.S. acknowledges support from the Australian Research Council (grant FT140100610). S.S. was supported by a University of Newcastle PhD scholarship. GR acknowledges support from University of Rosario's Science and Technology Secretary (grant ING509). Comments from Andrea D'Alpaos, Nicoletta Leonardi and two other anonymous reviewers helped improve the manuscript.

References

ABRANTES, K. & SHEAVES, M. 2009. Food web structure in a near-pristine mangrove area of the Australian Wet Tropics. *Estuarine, Coastal and Shelf Science,* 82**,** 597-607.

ARMITAGE, A. R., HIGHFIELD, W. E., BRODY, S. D. & LOUCHOUARN, P. 2015. The Contribution of Mangrove Expansion to Salt Marsh Loss on the Texas Gulf Coast. *PLOS ONE,* 10**,** e0125404.

BELLIARD J.-P., DI MARCO N., CARNIELLO L., TOFFOLON M. (2016) Sediment and vegetation spatial dynamics facing sea-level rise in microtidal salt marshes: Insights from an ecogeomorphic model, *Advances in Water Resources*, 93, 249-264.

BELLIARD, J. P., TOFFOLON, M., CARNIELLO, L. & D'ALPAOS, A. 2015. An ecogeomorphic model of tidal channel initiation and elaboration in progressive marsh accretional contexts. *Journal of Geophysical Research: Earth Surface,* 120**,** 1040-1064.

CARNIELLO, L., SILVESTRI, S., MARANI, M., D'ALPAOS, A., VOLPE, V. & DEFINA, A. 2014. Sediment dynamics in shallow tidal basins: In situ observations, satellite retrievals, and numerical modeling in the Venice Lagoon. *Journal of Geophysical Research: Earth Surface,* 119**,** 802-815.

BOON, P. I., ALLEN, T., CARR, G., FROOD, D., HARTY, C., MCMAHON, A., MATHEWS, S., ROSENGREN, N., SINCLAIR, S., WHITE, M. & YUGOVIC, J. 2015. Coastal wetlands of Victoria, south-eastern Australia: providing the inventory and condition information needed for their effective management and conservation. *Aquatic Conservation: Marine and Freshwater Ecosystems,* 25**,** 454-479.

CARNIELLO, L., D'ALPAOS, A. & DEFINA, A. 2011. Modeling wind waves and tidal flows in shallow micro-tidal basins. *Estuarine, Coastal and Shelf Science,* 92**,** 263-276.

CHEN, Y., LI, Y., CAI, T., THOMPSON, C. & LI, Y. 2016. A comparison of biohydrodynamic interaction within mangrove and saltmarsh boundaries. *Earth Surface Processes and Landforms,* 41**,** 1967-1979.

CHURCH, J. A., CLARK, P. U., CAZENAVE, A., GREGORY, J. M., JEVREJEVA, S., LEVERMANN, A., MERRIFIELD, M. A., MILNE, G. A., NEREM, R. S., NUNN, P. D., PAYNE, A. J., PFEFFER, W. T., STAMMER, D. & UNNIKRISHNAN, A. S. 2013. Sea Level Change. *In:* STOCKER, T. F., QIN, D., PLATTNER, G.-K., TIGNOR, M., ALLEN, S. K., BOSCHUNG, J., NAUELS, A., XIA, Y., BEX, V. & MIDGLEY, P. M. (eds.) *Climate Change 2013: The Physical Science Basis. Contribution of Working Group I to the Fifth Assessment Report of the Intergovernmental Panel on Climate Change.* Cambridge, United Kingdom and New York, NY, USA: Cambridge University Press.

CRAFT, C., CLOUGH, J., EHMAN, J., JOYE, S., PARK, R., PENNINGS, S., GUO, H. & MACHMULLER, M. 2009. Forecasting the effects of accelerated sea-level rise on tidal marsh ecosystem services. *Frontiers in Ecology and the Environment,* 7**,** 73-78.

CRASE, B., LIEDLOFF, A., VESK, P. A., BURGMAN, M. A. & WINTLE, B. A. 2013. Hydroperiod is the main driver of the spatial pattern of dominance in mangrove communities. *Global Ecology and Biogeography,* 22**,** 806-817.

CUNGE, J. A. 1975. Two dimenssional modeling of floodplains. *In:* MAHMOOD, K. & YEVJEVICH, V. (eds.) *Unsteady flow in open channels.* Colorado: Water Resources Publications.

D'ALPAOS, A., LANZONI, S., MARANI, M. & RINALDO, A. 2007. Landscape evolution in tidal embayments: Modeling the interplay of erosion, sedimentation, and vegetation dynamics. *Journal of Geophysical Research: Earth Surface,* 112, F01008.

D'ALPAOS, A., LANZONI, S., MUDD, S. M. & FAGHERAZZI, S. 2006. Modeling the influence of hydroperiod and vegetation on the cross-sectional formation of tidal channels. *Estuarine, Coastal and Shelf Science,* 69**,** 311-324.

D'ALPAOS, A. & MARANI, M. 2016. Reading the signature of biologic-geomorphic feedbacks in salt-marsh landscapes, *Advances in Water Resources,* 39, 265-275

D'ALPAOS, A., MUDD, S. M. & CARNIELLO, L. 2011. Dynamic response of marshes to perturbations in suspended sediment concentrations and rates of relative sea level rise, *J. Geophys. Res.*, 116, F04020, doi:10.1029/2011JF00209

DAY, J. W., CHRISTIAN, R. R., BOESCH, D. M., YÁÑEZ-ARANCIBIA, A., MORRIS, J., TWILLEY, R. R., NAYLOR, L., SCHAFFNER, L. & STEVENSON, C. 2008. Consequences of Climate Change on the Ecogeomorphology of Coastal Wetlands. *Estuaries and Coasts,* 31**,** 477-491.

DIETRICH, J. C., WESTERINK, J. J., KENNEDY, A. B., SMITH, J. M., JENSEN, R. E., ZIJLEMA, M., HOLTHUIJSEN, L. H., DAWSON, C., JR., R. A. L., POWELL, M. D., CARDONE, V. J., COX, A. T., STONE, G. W., POURTAHERI, H., HOPE, M. E., TANAKA, S., WESTERINK, L. G., WESTERINK, H. J. & COBELL, Z. 2011. Hurricane Gustav (2008) Waves and Storm Surge: Hindcast, Synoptic Analysis, and Validation in Southern Louisiana. *Monthly Weather Review,* 139**,** 2488-2522.

FAGHERAZZI, S., KIRWAN, M. L., MUDD, S. M., GUNTENSPERGEN, G. R., TEMMERMAN, S., D'ALPAOS, A., VAN DE KOPPEL, J., RYBCZYK, J. M., REYES, E., CRAFT, C. & CLOUGH, J. 2012. Numerical models of salt marsh evolution: Ecological, geomorphic, and climatic factors. *Reviews of Geophysics,* 50.

GEDAN, K. B., SILLIMAN, B. R. & BERTNESS, M. D. 2009. Centuries of Human-Driven Change in Salt Marsh Ecosystems. *Annual Review of Marine Science,* 1**,** 117-141.

HAYWARD, B. W., GRENFELL, H. R. & SCOTT, D. B. 1999. Tidal range of marsh foraminifera for determining former sea-level heights in New Zealand. *New Zealand Journal of Geology and Geophysics,* 42**,** 395-413.

HOWE, A. 2008. *Hydrodynamics, geomorphology and vegetation of estuarine wetlands in the Hunter, Australia: implications for migratory shorebird high tide roost availability.* PhD Thesis, University of Newcastle.

HOWE, A. J., RODRÍGUEZ, J. F. & SACO, P. M. 2009. Surface evolution and carbon sequestration in disturbed and undisturbed wetland soils of the Hunter estuary, southeast Australia. *Estuarine, Coastal and Shelf Science,* 84**,** 75-83.

HOWE, A. J., RODRIGUEZ, J. F., SPENCER, J., MACFARLANE, G. R. & SAINTILAN, N. 2010. Response of estuarine wetlands to reinstatement of tidal flows. *Marine and Freshwater Research,* 61**,** 702-713.

KELLEWAY, J. J., CAVANAUGH, K., ROGERS, K., FELLER, I. C., ENS, E., DOUGHTY, C. & SAINTILAN, N. 2017. Review of the ecosystem service implications of mangrove encroachment into salt marshes. *Global Change Biology* 23:3967–3983.

KELLEWAY, J. J., SAINTILAN, N., MACREADIE, P. I., SKILBECK, C. G., ZAWADZKI, A. & RALPH, P. J. 2016. Seventy years of continuous encroachment substantially increases 'blue carbon' capacity as mangroves replace intertidal salt marshes. *Global Change Biology,* 22**,** 1097-1109.

KIRWAN, M. L. & GUNTENSPERGEN, G. R. 2010. Influence of tidal range on the stability of coastal marshland. *Journal of Geophysical Research: Earth Surface,* 115**,** F02009.

KIRWAN, M. L., GUNTENSPERGEN, G. R., D'ALPAOS, A., MORRIS, J. T., MUDD, S. M. & TEMMERMAN, S. 2010. Limits on the adaptability of coastal marshes to rising sea level. *Geophysical Research Letters,* 37**,** .

KIRWAN, M. L. & MEGONIGAL, J. P. 2013. Tidal wetland stability in the face of human impacts and sea-level rise. *Nature,* 504**,** 53-60.

KIRWAN, M. L. & MURRAY, A. B. 2007. A coupled geomorphic and ecological model of tidal marsh evolution. *Proceedings of the National Academy of Sciences of the United States of America,* 104**,** 6118-6122.

KIRWAN, M. L. & MURRAY, A. B. 2008. Ecological and morphological response of brackish tidal marshland to the next century of sea level rise: Westham Island, British Columbia. *Global and Planetary Change,* 60**,** 471-486.

KIRWAN, M. L., TEMMERMAN, S., SKEEHAN, E. E., GUNTENSPERGEN, G. R. & FAGHERAZZI, S. 2016. Overestimation of marsh vulnerability to sea level rise. *Nature Climate Change,* 6**,** 253-260.

KRAUSS, K. W., MCKEE, K. L., LOVELOCK, C. E., CAHOON, D. R., SAINTILAN, N., REEF, R. & CHEN, L. 2014. How mangrove forests adjust to rising sea level. *New Phytologist,* 202**,** 19-34.

LOVELOCK, C. E., CAHOON, D. R., FRIESS, D. A., GUNTENSPERGEN, G. R., KRAUSS, K. W., REEF, R., ROGERS, K., SAUNDERS, M. L., SIDIK, F., SWALES, A., SAINTILAN, N., THUYEN, L. X. & TRIET, T. 2015. The vulnerability of Indo-Pacific mangrove forests to sea-level rise. *Nature,* 526**,** 559-563.

LUNDQUIST, C. J., MORRISEY, D. J., GLADSTONE-GALLAGHER, R. V. & SWALES, A. 2014. Managing Mangrove Habitat Expansion in New Zealand. *In:* FARIDAH-HANUM, I., LATIFF, A., HAKEEM, K. R. & OZTURK, M. (eds.) *Mangrove Ecosystems of Asia: Status, Challenges and Management Strategies.* New York, NY: Springer New York.

MACREADIE, P. I., OLLIVIER, Q. R., KELLEWAY, J. J., SERRANO, O., CARNELL, P. E., EWERS LEWIS, C. J., ATWOOD, T. B., SANDERMAN, J., BALDOCK, J., CONNOLLY, R. M., DUARTE, C. M., LAVERY, P. S., STEVEN, A. & LOVELOCK, C. E. 2017. Carbon sequestration by Australian tidal marshes. *Scientific Reports,* 7**,** 44071.

MAZDA, Y., WOLANSKI, E., KING, B., SASE, A., OHTSUKA, D. & MAGI, M. 1997. Drag force due to vegetation in mangrove swamps. *Mangroves and Salt Marshes* 1, 193–199.

MCKEE, K. L., CAHOON, D. R. & FELLER, I. C. 2007. Caribbean mangroves adjust to rising sea level through biotic controls on change in soil elevation. *Global Ecology and Biogeography,* 16**,** 545-556.

MORIASI, D. N., ARNOLD, J. G., VAN LIEW, M. W., BINGNER, R. L., HARMEL, R. D. & VEITH, T. L. 2007. Model evaluation guidelines for systematic quantification of accuracy in watershed simulations. *Transactions of the Asabe,* 50**,** 885-900.

MORRIS, J. T., SUNDARESHWAR, P. V., NIETCH, C. T., KJERFVE, B. & CAHOON, D. R. 2002. RESPONSES OF COASTAL WETLANDS TO RISING SEA LEVEL. *Ecology,* 83, 2869-2877.

MUDD, S. M., FAGHERAZZI, S., MORRIS, J. T. & FURBISH, D. J. 2004. Flow, Sedimentation, and Biomass Production on a Vegetated Salt Marsh in South Carolina: Toward a Predictive Model of Marsh Morphologic and Ecologic Evolution. *The Ecogeomorphology of Tidal Marshes.* American Geophysical Union.

NEAL, J., SCHUMANN, G. & BATES, P. 2012. A subgrid channel model for simulating river hydraulics and floodplain inundation over large and data sparse areas. *Water Resources Research,* 48**,** W11506.

OLIVER, T. S. N., ROGERS, K., CHAFER, C. J. & WOODROFFE, C. D. 2012. Measuring, mapping and modelling: an integrated approach to the management of mangrove and saltmarsh in the Minnamurra River estuary, southeast Australia. *Wetlands Ecology and Management,* 20**,** 353-371.

PASSERI, D. L., HAGEN S. C., MEDEIROS S. C., BILSKIE M. V., ALIZAD K., & WANG D. (2015), The dynamic effects of sea level rise on low-gradient coastal landscapes:A review, Earth's Future, 3, 159–181

RICCARDI, G. 2000. A cell model for hydrological-hydraulic modeling. *Journal of Environmental Hydrology,* 8.

RODRÍGUEZ, J. F. & HOWE, A. 2013. Estuarine Wetland Ecohydraulics and Migratory Shorebird Habitat Restoration. *Ecohydraulics.* John Wiley & Sons, Ltd.

RODRÍGUEZ, J. F., SACO, P. M., SANDI, S., SAINTILAN, N. & RICCARDI, G. 2017. Potential increase in coastal wetland vulnerability to sea-level rise suggested by considering hydrodynamic attenuation effects. *Nature Communications* 8**,** 16094.

ROGERS, K., SAINTILAN, N. & COPELAND, C. 2012. Modelling wetland surface elevation dynamics and its application to forecasting the effects of sea-level rise on estuarine wetlands. *Ecological Modelling,* 244**,** 148-157.

ROGERS, K., SAINTILAN, N., HOWE, A. J. & RODRÍGUEZ, J. F. 2013. Sedimentation, elevation and marsh evolution in a southeastern Australian estuary during changing climatic conditions. *Estuarine, Coastal and Shelf Science,* 133**,** 172-181.

SACO, P. M. & RODRÍGUEZ, J. F. 2013. 2.14 Modeling Ecogeomorphic Systems In: John F. Shroder (ed.) *Treatise on Geomorphology,* Volume 2, pp. 201-220. San Diego: Academic Press.

SAINTILAN, N. & ROGERS, K. 2013. The significance and vulnerability of Australian saltmarshes: implications for management in a changing climate. *Marine and Freshwater Research,* 64**,** 66-79.

SAINTILAN, N., ROGERS, K. & MCKEE, K. 2009. Salt Marsh-Mangrove Interactions in Australasia and the Americas. *In:* PERILLO, G. M. E., WOLANSKI, E., CAHOON, D. R. & BRINSON, M. M. (eds.) *Coastal Wetlands - An Integrated Ecosystem Approach.* The Netherlands: Elsevier Science.

SAINTILAN, N. & WILLIAMS, R. J. 1999. Mangrove Transgression into Saltmarsh Environments in South-East Australia. *Global Ecology and Biogeography,* 8**,** 117-124.

SAINTILAN, N., WILSON, N. C., ROGERS, K., RAJKARAN, A. & KRAUSS, K. W. 2014. Mangrove expansion and salt marsh decline at mangrove poleward limits. *Global Change Biology,* 20**,** 147-157.

SPIER, D., GERUM, H. L. N., NOERNBERG, M. A. & LANA, P. C. 2016. Flood regime as a driver of the distribution of mangrove and salt marsh species in a subtropical estuary. *Journal of Marine Systems,* 161**,** 11-25.

STENTA, H. R., RICCARDI, G. A. & BASILE, P. A. 2017. Grid size effects analysis and hydrological similarity of surface runoff in flatland basins. *Hydrological Sciences Journal,* 62**,** 1736-1754.

STRAW, P. & SAINTILAN, N. 2006. Loss of shorebird habitat as a result of mangrove incursion due to sea-level rise and urbanization *In:* BOERE, G. C., GALBRAITH, C. A. & STROUD, D. A. (eds.) *Waterbirds arounf the world: A*

global overview of the conservation management and research of the world's waterbird flyways. Edinburgh, UK: The Stationery Office Limited.

TAMBRONI, N. & SEMINARA, G. 2012. A one-dimensional eco-geomorphic model of marsh response to sea level rise: Wind effects, dynamics of the marsh border and equilibrium. *Journal of Geophysical Research: Earth Surface,* 117**,** F03026 .

TEMMERMAN, S., BOUMA, T. J., GOVERS, G., WANG, Z. B., DE VRIES, M. B. & HERMAN, P. M. J. 2005. Impact of vegetation on flow routing and sedimentation patterns: Three-dimensional modeling for a tidal marsh. *Journal of Geophysical Research: Earth Surface,* 110**,** .

TEMMERMAN, S., DE VRIES, M. B. & BOUMA, T. J. 2012. Coastal marsh die-off and reduced attenuation of coastal floods: A model analysis. *Global and Planetary Change,* 92–93**,** 267-274.

TEMMERMAN, S. & KIRWAN, M. L. 2015. Building land with a rising sea. *Science,* 349**,** 588-589.

TEMMERMAN, S., MEIRE, P., BOUMA, T., HERMAN, P., YSEBAERT, T. & DE VRIEND, H. 2013. *Ecosystem-based coastal defence in the face of global change*. *Nature,* 504, 79–83.

VAN WIJNEN, H. J. & BAKKER, J. P. 2001. Long-term Surface Elevation Change in Salt Marshes: a Prediction of Marsh Response to Future Sea-Level Rise. *Estuarine, Coastal and Shelf Science,* 52**,** 381-390.

WARD, R. D., FRIESS, D. A., DAY, R. H. & MACKENZIE, R. A. 2016. Impacts of climate change on mangrove ecosystems: a region by region overview. *Ecosystem Health and Sustainability,* 2**,** e01211-n/a.

WILLIAMS, R. J. & WATFORD, F. A. 1997. Identification of structures restricting tidal flow in New South Wales, Australia. *Wetlands Ecology and Management,* 5**,** 87-97.

WILLIAMS, R. J., WATFORD, F. A. & BALASHOV, V. 2000. Kooragang Wetland Rehabilitation Project: History of Cahnges to Estuarine Wetlands of the Lower Hunter River. *NSW Final Report Series.* Cronulla, Australia: NSW Fisheries Office of Conservation.

WINEMILLER, K. O., AKIN, S. & ZEUG, S. C. 2007. Production sources and food web structure of a temperate tidal estuary: integration of dietary and stable isotope data. *Marine Ecology Progress Series,* 343**,** 63-76.

WOODROFFE, C. D., ROGERS, K., MCKEE, K. L., LOVELOCK, C. E., MENDELSSOHN, I. A. & SAINTILAN, N. 2016. Mangrove Sedimentation and Response to Relative Sea-Level Rise. *Ann Rev Mar Sci,* 8**,** 243-66.

YAMAZAKI, D., KANAE, S., KIM, H. & OKI, T. 2011. A physically based description of floodplain inundation dynamics in a global river routing model. *Water Resources Research,* 47**,** W04501.